Programable lattices of optical vortices in nematic liquid crystal

R. Barboza[a,c], G. Assanto[b],U. Bortolozzo[a], M.G. Clerc[c], S. Residori[a] and E. Vidal-Henriquez [c]

[a]INLN, Université de Nice-Sophia Antipolis, CNRS, 1361 Route des Lucioles, 06560 Valbonne, France;
[b] NooEL-Nonlinear Optics and OptoElectronics Lab, University Roma Tre, Via della Vasca Navale 84, 00146 Rome, Italy;
[c]Departamento de Física, FCFM, Universidad de Chile, Casilla 487-3, Santiago, Chile.

ABSTRACT

Using self-induced vortex-like defects in the nematic liquid crystal layer of a light valve with photo-sensible wall, we demonstrate the realization of programable optical vortices lattices with arbitrary configuration in space. On each lattice site, every matter vortex acts as a photonic spin-to-orbital momentum coupler and an array of circularly polarized input beams is converted into an output array of vortex beams with topological charges consistent with the vortex matter lattice. The vortex arrangements are explained the basis of light-induced matter defects and topological rules.

Keywords: Optical vortex, Umbilical defects, Optical lattice.

1. INTRODUCTION

Optical vortices consist in singular points where the electromagnetic field goes to zero and around which the phase distribution forms an n-armed spiral, with n the topological charge.[1–3] In low-order Gauss-Laguerre beams, a single optical vortex corresponds to a phase singularity on the beam axis. Vortex beams attract a lot of attention in view of their diverse photonic applications,[4] including the exchange of angular momentum between light and matter,[5] optical tweezers,[6–8] quantum computation,[9] data transmission[10] and enhancement of astronomical images.[11] To date, optical vortices were generated mainly by using spiral phase plates[12] or diffractive elements.[13] Recently, the introduction of q-plates, planar elements with a pre-set radial director orientation in nematic liquid crystals, has opened new promising avenues,[14] as well as the exploitation of umbilic-like defects in nematic textures.[15] This approach provides both tunability and high efficiency, although the liquid crystal alignment can cause some beam deformation and a consequent degradation of the generated optical vortices if it is not done properly.[16] Particularly, the alignment of the incoming beam with the "vortex-making" element remains critical in certain conditions, for instance, in the presence of atmospheric turbulence as required by coronagraph applications[17] or astronomical imaging.[11] Recently, by exploiting reorientational nonlinearities in the nematic liquid crystal layer of a light-valve we have realized the optically addressed self-induction of vortex-beams that are self-aligned with the impinging light beam.[18]

We show that a similar approach can be successfully exploited to create closely packed lattices of optical vortices with arbitrary and reconfigurable geometric distributions.[19] As long as nematic liquid crystal reorientation occurs only in the illuminated areas—which happens for relatively low amplitudes of the voltage applied to the light-valve—the vortices on adjacent lattice sites are independent from one another and all have the same sign. Increasing the applied voltage, reorientation occurs in the whole liquid crystal layer and all the vortices become tightly coupled together, leading to the spontaneous generation of defects with opposite sign in between adjacent lattice sites. The resulting vortex arrangement is consistent with topologic conservation rules accounting for the reconnection of reorientation lines in the distorted nematic layer.[2] Similar rules were recently reported with

Further author information: (Send correspondence to M.G.C.)
M.G.C.: E-mail: marcel@dfi.uchile.cl, Telephone: 562 2978 4676

Liquid Crystals XIX, edited by Iam Choon Khoo, Proc. of SPIE Vol. 9565, 95650L
© 2015 SPIE · CCC code: 0277-786X/15/$18 · doi: 10.1117/12.2185512

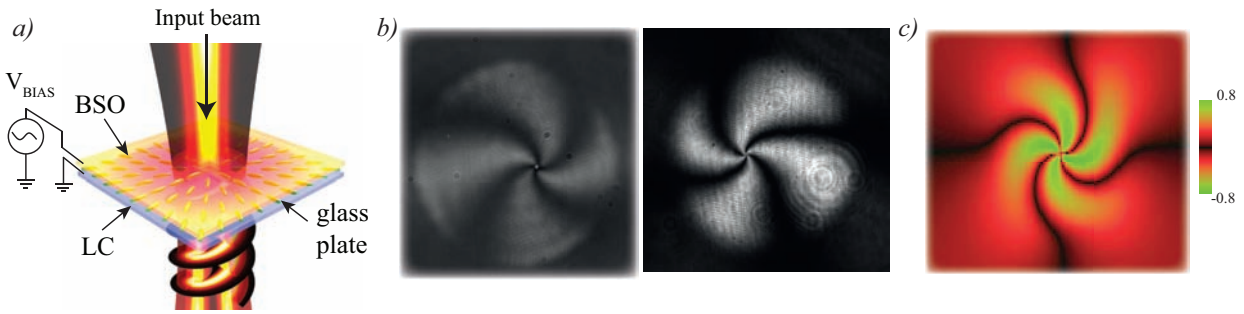

Figure 1. a) Schematic representation of optically addressed vortex induction in a liquid crystal light valve. b) Typical matter defects, umbilicals, observed under crossed polarizers with different bias tension. c) Vortex solutions of the forced Ginzburg-Landau Equation(4).

reference to topological colloids, where particles of various shapes were introduced in a nematic liquid crystal host,[20] as well as in homeotropically aligned nematic samples when submitted to magnetic fields created by small magnets.[21] Remarkably enough, in our case all the topological reconnections are reconfigurable, optically addressable, and tunable via the electric field applied to the light-valve. Moreover, the induced defect lattices act as arrays of photonic spin-to-orbital angular momentum couplers with both signs of the topological charge. For a circularly polarized input beam, the matter vortex at each lattice site generates a Laguerrre-Gauss output beam with topological charge determined by the sign of the defect and the spin-to-orbital angular momentum transfer.

2. EXPERIMENTAL SETUP

The vortex induction process is schematically represented in Fig.1. The liquid crystal light valve (LCLV) is filled with a nematic mixture exhibiting negative dielectric anisotropy, $\Delta\varepsilon = \varepsilon_{//} - \varepsilon_{\perp} < 0$. In such valve, the transparent interfaces are treated in order to provide an homeotropic alignment to the liquid crystals, that is, with the nematic director (optic axis) perpendicular to the confining walls, one of which is a photoconductive $Bi_{12}SiO_{20}$ (BSO) slab. Owing to this photoconductive substrate, when the LCLV is illuminated by a Gaussian light beam, the effective voltage drop across the LC layer acquires a bell shaped profile, peaked in the centre of the illuminated area and are able to overcome the critical value of the Fréderickszs transition in this area, for which the elongated molecules start to reorient owing to the torque exerted by the electric field on the induced dipoles.[22] Since we employ a liquid crystal with negative (low frequency) dielectric anisotropy, the torque exerted along the short molecular axis is larger than that on the long axis, therefore, the molecules tend to (re)align perpendicularly to the electric field, leading to a 2π-degenerate reorientation and the formation of topological defects in the nematic texture.[23]

To understand the mechanism of the optical vortex self-induction, we consider the effect of the illumination of the LCLV with a Gaussian beam, which induces a voltage drop with a bell-shaped profile across the liquid crystal layer, higher in the center of the illuminated area. In order to determine the voltage drop shape within the sample, one can model the sample as consisting of two infinitely extended planar parallel plates separated by d. z accounts for the coordinate orthogonal to the plates. The upper plate, located in $z = d$, is illuminated

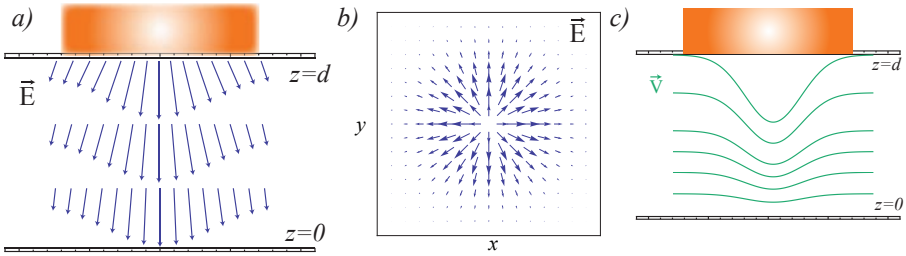

Figure 2. a-b) Electric field $\vec{E}$ and c) voltage $V(x, y, z)$ inside the LC light-valve.

by the Gaussian beam. after introducing cylindrical coordinates, the voltage $V(r,\theta,z)$ satisfies the Laplace equation $\partial_{zz}V + \frac{\varepsilon_\perp}{\varepsilon_{//}}\nabla_\perp^2 V = 0$, where $\nabla_\perp^2$ is the Laplacian operator in polar coordinates, $\varepsilon_\perp$ and $\varepsilon_{//}$ are the dielectric constants perpendicular and parallel to the nematic director, respectively. The voltage satisfies the boundary conditions in the respective plates $V(z=d) = V_0 + \alpha I(r)$, and $V(z=0) = 0$, where $I(r)$ stands for the intensity of Gaussian beam, $I(r) = I_0 e^{-r^2/\omega^2}$. I_0 is the peak intensity and ω the waist, respectively. Using the Fourier transform in polar coordinates and solving the above Lapalce equation with the corresponding boundary conditions, after straightforward calculations one obtains

$$V(z,r) = \frac{1}{2\pi}\int_{-\infty}^{\infty} \mathrm{d}k e^{-ik\cdot r_\perp} \frac{\sinh\left(\sqrt{\frac{\varepsilon_\perp}{\varepsilon_\parallel}}kz\right)}{\sinh\left(\sqrt{\frac{\varepsilon_\perp}{\varepsilon_\parallel}}kd\right)} \left(\int_0^{\infty} \mathrm{d}r_\perp^* e^{ik\cdot r_\perp^*}[V_0 + \alpha I(r_\perp^*/\omega)]\right). \quad (1)$$

This expression is an exact analytical solution, however it is intricated to infer results from it. For the sake of simplicity, we consider a Gaussian beam sufficiently flattened ($\omega \to \infty$) so that the above expression to the dominant order takes the form $V(z,r) \approx \frac{z}{d}[V_0 + \alpha I(r/\omega)]$. The first and second terms on the right hand side account for the voltage drop due to, respectively, the externally applied bias and the voltage drop induced by the Gaussian beam impinging on the sample. Figure 2b illustrates the voltage drop inside the LCLV. Then, the electric field $\vec{E}(r,\theta,z)$ inside the LCLV takes the form

$$\vec{E} = -\nabla V = E_z\hat{z} + E_r\hat{r} = -\frac{1}{d}\left[V_0 + \alpha I(r/\omega)\right]\hat{z} - \frac{z\alpha}{d\omega}\frac{dI(r/\omega)}{dr}\hat{r}, \quad (2)$$

with $\hat{z}$ and $\hat{r}$ the unitary vectors in cylindrical coordinates. Figure 2a shows the profile of the electric field inside the LCLV. Hence, if the incoming light beam has a Gaussian profile, it also produces a transverse component of the electric field, thus giving rise to an effective potential able to create a topological defect and pin it close to the optical intensity peak.[18] The created defect, in turn, couples orbital and spin components of the optical

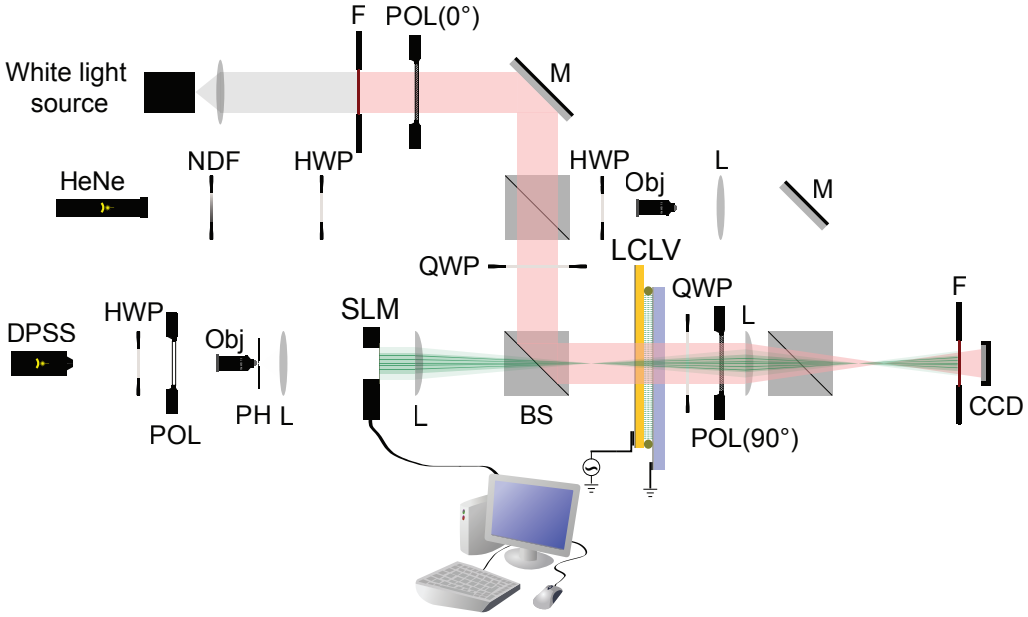

Figure 3. Experimental setup to create optical vortex lattice. OBJ: objective; BS: beam splitter; M: mirror; SLM: spatial light modulator; NDF: neutral density filter; F: red filter; POL: polarizer; HWP: half-wave plate; QWP: quarter-wave plate; PH: pinhole; L: lens; CCD: charge-coupled device camera. Bottom inset: example of square modulation mask as input to the SLM. Upper inset: Enlarged view of the sample observed under crossed polarizers when illuminated with the square grid (bright spots from the DPSS green laser) and white light background; on the left an enlarged view of a single vortex.

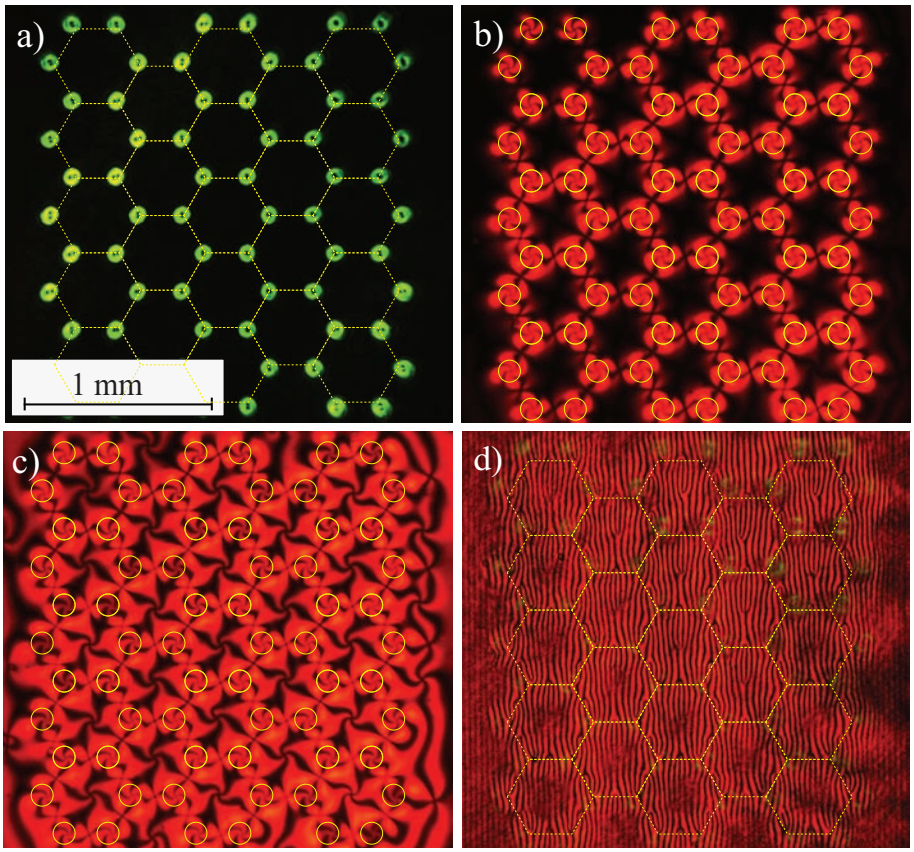

Figure 4. Hexagonal vortex lattices. a) Laser intensity distribution, $V = 19\ V$; b-c) white light images under crossed polarizers, b) independent vortices, $V = 18\ V$, c) fully coupled vortex lattice, $V = 22\ V$; d) interferogram of the vortex lattice, $V = 12\ V$; the dashed lines mark the lattice structure, the circles indicate the positions of the addressing light spots. The input intensity is $I = 250\ \mu W/cm^2$.

angular momentum; hence, the outgoing beam acquires a helical wavefront. The experimental characterization of the matter defect was initially carried out by observing it under crossed polarizers, as shown in the left panel of Fig.1b. The black cross appearing in these conditions is the signature of a umbilic-like defect.[24]

3. MODEL

The presence of an inhomogeneous electric field strongly modifies the dynamics of the LC director $\vec{n}$. The dynamical equation for the molecular director $\vec{n}$ reads[22,25]

$$\gamma\partial_t\vec{n} = K_3[\nabla^2\vec{n} - \vec{n}(\vec{n}\cdot\nabla^2\vec{n})] + (K_3 - K_1)[\vec{n}(\vec{n}\cdot\vec{\nabla})(\vec{\nabla}\cdot\vec{n}) - \vec{\nabla}(\vec{n}\cdot\vec{\nabla})]$$

$$+2(K_2 - K_3)[(\vec{n}\cdot\vec{\nabla}\times\vec{n})(\vec{n}(\vec{n}\cdot\vec{\nabla}\times\vec{n}) - \vec{\nabla}\times\vec{n}) + \vec{n}\times\vec{\nabla}(\vec{n}\cdot\vec{\nabla}\times\vec{n})] + \Delta\varepsilon(\vec{n}\cdot\vec{E})[\vec{E} - \vec{n}(\vec{n}\cdot\vec{E})], \qquad (3)$$

where γ is the relaxation time, $\{K_1, K_2, K_3\}$ are the nematic LC elastic constants.[22] The dynamics of the director is of relaxation type and is characterised by preserving the norm of the director. The homeotropic state, $\vec{n} = \hat{z}$, undergoes a stationary instability for critical values of the voltage $V_0 \equiv V_{FT} = \sqrt{-K_3\pi^2/\Delta\varepsilon}$, which correspond to the Fréedericksz transition.[22,25] Close to this transition point and considering the inhomogeneous electric field $\vec{E}(r,\theta,z)$, to dominant order one can use the following ansatz for the amplitude of the critical mode

$$\vec{n}(r,\theta,z) \approx \begin{pmatrix} u(r,\theta,t)\sin(\frac{\pi z}{d}) \\ w(r,\theta,t)\sin(\frac{\pi z}{d}) \\ 1 - \frac{(u^2+w^2)}{2}\sin^2(\frac{\pi z}{d}) \end{pmatrix}.$$

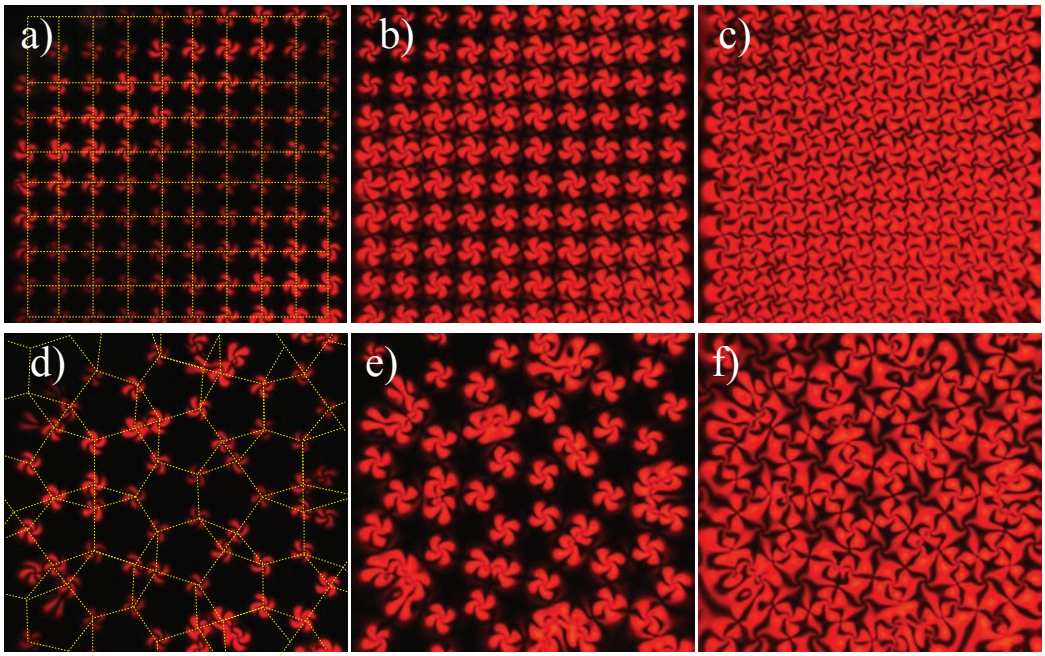

Figure 5. Vortex lattices with various spatial distributions; images are taken through crossed polarizers. Squares for a-c) $V = 14, 18, 22\ V_{rms}$; and Penrose lattice for d-f) $V = 14, 18, 22\ V_{rms}$; the dashed lines mark the corresponding lattice structures. The addressing light intensity is $I = 250\ \mu W/cm^2$ in all cases.

Introducing the above ansatz in the director equation, integrating in the z coordinate over one period, and considering the complex amplitude $A \equiv u + iw$ is the amplitude of the LC director field deformation, after straightforward calculations one obtains forced Ginzburg-Landau (GL) equation

$$\gamma \partial_t A = \mu A - aA|A|^2 + K\nabla_\perp^2 A + \delta \partial_{\eta,\eta} \bar{A} + b\frac{E_r(z)}{z} E_z e^{i\theta} \tag{4}$$

where $\mu \equiv -K_3 k^2 - \Delta\varepsilon E_z^2(r,z)$ is the bifurcation parameter describing the Fréedericksz transition, $a \equiv -(K_3 k^2/4 + 3\Delta\varepsilon E_z^2/4) > 0$ is the saturation parameter, $b \equiv \Delta\varepsilon 2d/\pi$, $\partial_\eta \equiv \partial_x + i\partial_y$, $\nabla_\perp \equiv \partial_{\eta,\bar{\eta}}$, $K \equiv (K_1 + K_2)/2$, and $\delta \equiv (K_1 - K_2)/2$ accounts for the elastic anisotropy. Without the last two terms, the above equation is the well-know GL equation, which is a prototype model widely employed to describe dissipative vortex dynamics.[2] The inclusion of the last two terms account for the elastic anisotropy of the liquid crystal and the effective electric potential induced by the light impinging on the photoconductor, which are responsible for the pinning of the matter vortex at the center of the illuminated area.[18,19] The last term on the right hand side is an external forcing generated by the inhomogeneous radial electric field. Such forcing term is responsible for inducing a matter vortex with positive charge in the center position where the applied Gaussian beam is peaked, which is at the origin of the self-stabilization mechanism. The anisotropic term—term proportional to δ—is responsible for moving and slightly rotating the matter vortex. Figure 1c shows numerical simulations of this model and the comparison with a matter vortex experimentally obtained.

Therefore, we have established that a beam of light impinging on the liquid crystal light valve induces simultaneously an optical vortices in the matter (umbilical defect), and turn on the light (optical vortex). Then, from this mechanism, one can create vortex lattices of matter and light by using different light rays applied to the LCLV.

The setup for generating vortex lattices is sketched in Fig. 3. The beam of a diode-pumped frequency-doubled solid-state (DPSS) laser at wavelength $\lambda = 532\ nm$ is expanded, collimated and directed to a spatial light modulator (SLM). The SLM is computer driven by intensity masks (an example is shown in the inset, the lattice period is 0.5 mm, the diameter of the vortex core is 1.2 μm) which, through a lens, are imaged onto the BSO side of the LCLV. The vortex beams at the LCLV output are recorded by a CCD camera. In order to

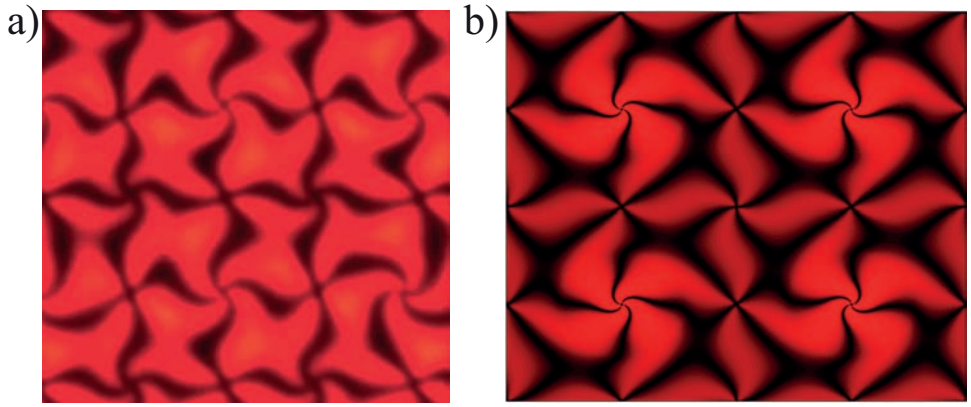

Figure 6. Square optical lattice, a) experimental lattice with $V = 22$ Vrms and intensity is $I = 250\ \mu\mathrm{W/cm}^2$, b) numerical simulation of the forced Ginzburg-Landau Eq. (4) with $\mu = 2$, $\delta = 0.7$, $K = 1$, and $a = 1$.

observe the whole orientational structure inside the LC layer, the LCLV can also be illuminated by white light and the transmitted field imaged at the CCD plane. Polarizers and red filters discriminate the green vortex beams from the white light transmitted through the valve. A He-Ne laser at wavelength $\lambda = 632\ nm$ is used to realize an interferometer, through which the phase singularities are visualized by making the whole vortex lattice interfere with an expanded collimated beam.

Defect lattices were generated with various symmetries and spatial configurations, specifically designing the intensity masks for the SLM in order to achieve close packing of the vortices. Examples of hexagonal vortex lattices are displayed in Fig.4. At low voltage, the vortices are independent from one another and can be individually addressed (Fig.4a-b). When the voltage is increased, adjacent vortices become coupled through reorientation in the whole nematic background. Because of the topological constraints associated to the reconnection of reorientation lines, two (initially generated) adjacent vortices of equal sign induce a vortex of opposite charge in between them. An example of fully connected network of vortices with alternating signs is visible in Fig.4c.

Employing suitably designed intensity masks, we realized vortex lattices with several configurations, as shown in Figure 5 for squares and Penrose lattice. Again, as the bias was increased from low to high voltages, we could observe the transition from independent vortices to a fully connected network of adjacent vortices of alternating signs.

Figure 6 displays a numerical simulation of the vortex lattice structure obtained by using the forced anisotropic Ginzburg-Landau model, Eq.(4), and its respective comparison with an experimental square vortex lattice. This numeric lattice is accomplished by applying a Gaussian forcing distributed with a square lattice structure. Qualitatively, both lattices show similar properties.

4. CONCLUSIONS

In conclusion, we have shown that reconfigurable optical vortex lattices in soft matter can be realized by self-induction of vortex-like defects in a nematic liquid crystal light-valve. The optical vortices are driven by their matter counterparts in the nematic texture, where umbilic-like defects are created in closely packed configurations of various geometrical distributions. Every defect on each lattice sites acts as a spin-to-orbital momentum coupler and can be harnessed either via optical addressing or by tuning the electric field applied to the light valve. These novel photonic structures in soft matter, easily reconfigurable and self-healing, can encompass the parallel processing of a large number of optical signals in two-dimensional arrays.

ACKNOWLEDGMENTS

UB, SR and MGC acknowledge financial support from the ANR international program, project ANR-2010-INTB-402-02 (ANR-CONICYT39), “COLORS” and FONDECYT No. 1120320. GA acknowledge travel funding from the Internationalization Program of University Roma Tre. E.V-H. thanks CONICYT-PCHA/Magíster Nacional/2013 - 221320023.

REFERENCES

[1] Nye, J. F. and Berry, M., "Dislocations in wave trains," *Proc. R. Soc. Lond. A* **336**, 165 (1974).

[2] Pismen, L. M., [*Patterns and Interfaces in Dissipative Dynamics*], Springer Series in Synergetics, Berlin Heidelberg (2006).

[3] Soskin, M. S. and Vasnetov, M. V., [*Singular Optics*], Prog. Opt. **42**, 219 (2001).

[4] Desyatnikov, A. S., Kivshar, Y. S., and Torner, L., [*Optical Vortices and Vortex Solitons*], Prog. Opt. **47**, 291 (2005).

[5] Allen, L., Beijersbergen, M. W., Spreeuw, R. J. C., and Woerdman, J. P., "Orbital angular momentum of light and the transformation of laguerre-gaussian laser modes," *Phys. Rev. A* **45**, 8185–8189 (Jun 1992).

[6] Grier, D. G., "A revolution in optical manipulation," *Nature* **424**, 810 (2003).

[7] Shvedov, V. G., Rode, A. V., Izdebskaya, Y. V., Desyatnikov, A. S., Krolikowski, W., and Kivshar, Y. S., "Giant optical manipulation," *Phys. Rev. Lett.* **105**, 118103 (Sep 2010).

[8] Padgett, M. and Bowman, R., "Tweezers with a twist," *Nature Photon.* **5**, 342 (2011).

[9] Arnaut, H. H. and Barbosa, G. A., "Orbital and intrinsic angular momentum of single photons and entangled pairs of photons generated by parametric down-conversion," *Phys. Rev. Lett.* **85**, 286–289 (Jul 2000).

[10] Wang, J., Yang, J.-Y., I. M. Fazal, a. N. A., Yan, Y., Huang, H., Ren, Y., Yue, Y., Dolinar, S., Tur, M., and Willner, A. E., "Terabit free-space data transmission employing orbital angular momentum multiplexing," *Nature Photon.* **6**, 488 (2012).

[11] Tamburini, F., Anzolin, G., Umbriaco, G., Bianchini, A., and Barbieri, C., "Overcoming the rayleigh criterion limit with optical vortices," *Phys. Rev. Lett.* **97**, 163903 (Oct 2006).

[12] M.W. Beijersbergen, L. Allen, H. v. d. V. J. W., "Astigmatic laser mode converters and transfer of orbital angular momentum," *Opt. Commun.* **96**, 123 (1993).

[13] Bazhenov, V. Y., Vasnetsov, M. V., and Soskin, M. S., "Laser beams with screw dislocations in their wavefronts," *JETP Lett.* **52**, 429 (1990).

[14] Marrucci, L., Manzo, C., and Paparo, D., "Optical spin-to-orbital angular momentum conversion in inhomogeneous anisotropic media," *Phys. Rev. Lett.* **96**, 163905 (Apr 2006).

[15] Brasselet, E., "Tunable optical vortex arrays from a single nematic topological defect," *Phys. Rev. Lett.* **108**, 087801 (Feb 2012).

[16] Bekshaev, A. Y. and Sviridova, S. V., "Effects of misalignments in the optical vortex transformation performed by holograms with embedded phase singularity," *Opt. Commun.* **283**, 4866 (2010).

[17] E. Serabyn, D. M. and Burruss, R., "An image of an exoplanet separated by two diffraction beamwidths from a star," *Nature* **464**, 1018 (2010).

[18] Barboza, R., Bortolozzo, U., Assanto, G., Vidal-Henriquez, E., Clerc, M. G., and Residori, S., "Vortex induction via anisotropy stabilized light-matter interaction," *Phys. Rev. Lett.* **109**, 143901 (Oct 2012).

[19] Barboza, R., Bortolozzo, U., Assanto, G., Vidal-Henriquez, E., Clerc, M. G., and Residori, S., "Harnessing optical vortex lattices in nematic liquid crystals," *Phys. Rev. Lett.* **111**, 093902 (Aug 2013).

[20] Senyuk, B., Liu, Q., He, S., and R. D. Kamien, R. B. Kusner, T. C. L. I. S., "Topological colloids," *Nature* **493**, 200 (2013).

[21] Pieranski, P., Yang, B., Burtz, L., Camu, A., and Simonetti, F., "Generation of umbilics by magnets and flows," *Liq. Cryst.* **12**, 1593–1608 (2013).

[22] de Gennes, P. G. and Prost, J., [*The Physics of Liquid Crystals*], Oxford Science Publications, Clarendon Press, 2nd edition (1993).

[23] Barboza, R., Sauma, T., Bortolozzo, U., Assanto, G., Clerc, M. G., and Residori, S., "Characterization of vortex pair interaction law and nonlinear," *New J. Phys.* **15**, 013028 (2013).

[24] Chandrasekhar, S., [*Liquid crystals*], Cambridge University Press, New York (1977).

[25] Khoo, I.-C. and Wu, S.-T., [*Optics and nonlinear optics of liquid crystals*], no. 1, World Scientific (1993).